Insertion of Nitriles into a Zirconium−Iridium Heterobimetallic Complex: A Mechanistic Study

J. Robin Fulton, Tracy A. Hanna, and Robert G. Bergman*

Department of Chemistry, University of California, Berkeley, California 94720

Received October 4, 1999

The reaction of $Cp_2Zr(\mu\text{-N-}^t\text{Bu})IrCp^*$ (**1**) with nitriles (RC≡N) yields the cyclometalated species $Cp_2Zr(\mu\text{-N-}^t\text{Bu})(\mu\text{-NC(H)(R)CH}_2\text{-}\eta^5\text{-}C_5Me_4)Ir$ (R = C_6H_5 (**2a**), *o*-Et-C_6H_4 (**2b**), (*p*-CH_3)-C_6H_4 (**2c**), (*p*-CF_3)C_6H_4 (**2d**), (*p*-MeO)C_6H_4 (**2e**), cyclopropyl (**2f**), $CH(Me)_2$ (**2g**), $NC(CH_2)_3$ (**2h**)). An intermediate is observed in the reaction of **1** with cyanocyclopropane. This intermediate has been characterized by NMR spectroscopy as a tetramethylfulvene complex with a bridging alkylidene−amido moiety, $Cp_2Zr(\mu\text{-N-}^t\text{Bu})(\mu\text{-NCRH})(\eta^5\text{-}C_5Me_4CH_2)Ir$ (R = cyclopropyl; **3**). Kinetic simulations were performed and provided evidence that the intermediate is productive. The reaction of **1** with 2-arylacetonitriles yields two noninterconvertible complexes: a cyclometalated species (**4**), analogous to complex **2**, and the new olefinic species $Cp_2Zr(\mu\text{-N-}^t\text{Bu})(\mu\text{-N-CHCH(R)}IrCp^*$ (R = C_6H_5 (**5a**), R = (*p*-CF_3)C_6H_4 (**5b**), R = (*p*-MeO)C_6H_4 (**5c**)). The reaction pathways for the formation of both **4** and **5** proceed through the fulvene complex **3**; however, the product ratio **5**:**4** was found to be dependent upon the reaction conditions.

Introduction

It has often been suggested that early−late heterobimetallic (ELHB) complexes, containing an early transition metal (from the left side of the transition-metal series) and a late transition metal (from the right side of the transition-metal series), might show novel reactivity compared with that of related mononuclear complexes.[1−22] One impetus for the study of ELHB complexes is the prospect of using them to induce carbon−heteroatom (C−Y; Y = N, O, S, P) bond cleavage in organic molecules. Since C−Y bonds are polarized, one might expect an electron-poor early-transition-metal center to react at the heteroatom and a more electron-rich late-transition-metal center to bond to the more electropositive carbon atom.[1,12] However, this type of cooperative reactivity between the metal centers was rarely observed until recently.[2,4−6,9,10,16,17,19,22] Most known ELHB complexes react at only one of the metal centers, while the second metal acts as a spectator atom.[1,3,15]

We recently reported the synthesis of the unique ELHB complex $Cp_2Zr(\mu\text{-N-}^t\text{Bu})IrCp^*$ (**1**; Cp = cyclopentadienyl, Cp* = pentamethylcyclopentadienyl).[4−6,9,10]

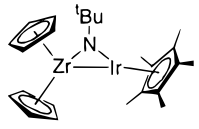

1

This compound is the first example of an ELHB imido complex and is the first structurally characterized complex to possess a Zr−Ir bond. Compound **1** also contains two electronically unsaturated metal centers (Zr = 16 e$^-$, Ir = 16 e$^-$) which makes the material an ideal candidate for cooperative reactivity. Indeed, reaction of **1** with a variety of carbon−heteroatom bonds results in cleavage of the metal−metal bond and thus involves both metal centers.[9,10] For instance, compound **1** reacts with carbon dioxide to produce a metallacyclo-

(1) Stephan, D. W. *Coord. Chem. Rev.* **1989**, *95*, 41−107.
(2) Casey, C. P. *J. Organomet. Chem.* **1990**, *400*, 205.
(3) Aubart, M. A.; Bergman, R. G. *J. Am. Chem. Soc.* **1996**, *118*, 1793.
(4) Baranger, A. M.; Hollander, F. J.; Bergman, R. G. *J. Am. Chem. Soc.* **1993**, *115*, 7890.
(5) Baranger, A. M.; Bergman, R. G. *J. Am. Chem. Soc.* **1994**, *116*, 3822.
(6) Baranger, A. M.; Hanna, T. A.; Bergman, R. G. *J. Am. Chem. Soc.* **1995**, *117*, 10041.
(7) Ferguson, G. S.; Wolczanski, P. T.; Paranyi, L.; Zonnevylle, M. C. *Organometallics* **1988**, *7*, 1967.
(8) Gelmini, L.; Stephan, D. W. *Organometallics* **1988**, *7*, 849.
(9) Hanna, T. A.; Baranger, A. M.; Bergman, R. G. *J. Am. Chem. Soc.* **1995**, *117*, 11363.
(10) Hanna, T. A.; Baranger, A. M.; Bergman, R. G. *Angew. Chem.* **1996**, *108*, 693.
(11) Hostetler, M. J.; Butts, M. D.; Bergman, R. G. *J. Am. Chem. Soc.* **1993**, *115*, 2743.
(12) Jansen, G.; Schubart, M.; Findeis, B.; Gade, L. H.; Scowen, I. J.; McPartlin, M. *J. Am. Chem. Soc.* **1998**, *120*, 7239.
(13) Mitani, M.; Hayakawa, M.; Yamada, T.; Teruaki, M. *Bull. Chem. Soc. Jpn.* **1996**, *69*, 2967.
(14) Ohff, A.; Zippel, T.; Arndt, P.; Spannenberg, A.; Kempe, R.; Rosenthal, U. *Organometallics* **1998**, *17*, 1649.
(15) Ozawa, F.; Park, J. W.; Mackenzie, P. B.; Schaefer, W. P.; Henling, L. M.; Grubbs, R. H. *J. Am. Chem. Soc.* **1989**, *111*, 1319.
(16) Pinkes, J. R.; Tetrick, S. P.; Landrum, B. E.; Cutler, A. R. *J. Organomet. Chem.* **1998**, *566*, 1.
(17) Schneider, A.; Gade, L. H.; Breuning, M.; Bringmann, G.; Scowen, I. J.; McPartlin, M. *Organometallics* **1998**, *17*, 1643.
(18) Zippel, T.; Arndt, P.; Ohff, A.; Spannenberg, A.; Kempe, R.; Rosenthal, U. *Organometallics* **1998**, *17*, 4429.
(19) Schubart, M.; Mitchell, G.; Gade, L. H.; Kottke, T.; Scowen, I. J.; McPartlin, M. *Chem. Commun.* **1999**, 233.
(20) Nakahara, N.; Hirano, M.; Fukuoka, A.; Komiya, S. *J. Organomet. Chem.* **1999**, *572*, 81.
(21) Lang, H.; Kohler, K.; Rheinwald, G.; Zaolnai, L.; et al. *Organometallics* **1999**, *18*, 598.
(22) Fabre, S.; Findeis, G.; Trosch, J. M.; Gade, L. H.; Scowen, I. J.; McPartlin, M. *Chem. Commun.* **1999**, 577.

10.1021/om990785l CCC: $19.00
Publication on Web 01/27/2000

pentane that incorporates a bridging metallacycle ester moiety (eq 1).[9]

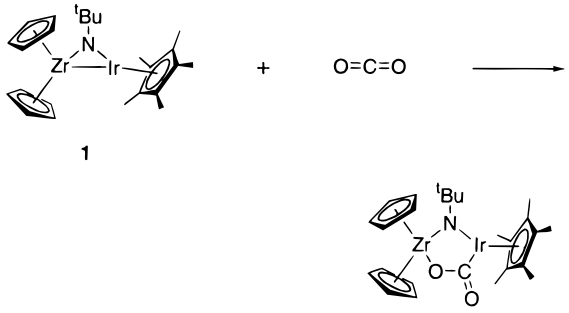

(1)

We wanted to explore the reactivity of **1** with other carbon−heteroatom multiple bonds, and thus we treated **1** with benzonitrile, expecting to observe a product similar to that in eq 1. Instead, the product that we observed was unusual. This led us to perform a detailed study on the mechanism of the reaction of **1** with nitriles. This paper describes the study and is organized into two parts. The first details the reaction of **1** with cyanoarenes and cyanoalkanes. A metastable intermediate in this process is observed and characterized by NMR spectroscopy. The second part describes the addition of 2-arylacetonitriles to **1**. Two noninterconvertible products are formed, one of which is analogous to the product formed in the reaction of **1** with cyanoalkanes and cyanoarenes. The product distribution was found to be a function of both temperature and concentration. Several perplexing mechanistic questions raised by these observations are discussed.

Results

Reaction of $Cp_2Zr(\mu$-N-^{t}Bu)IrCp* (1) with Cyanoarenes. Addition of a stoichiometric amount of benzonitrile in benzene to **1** results in the formation a dark green solution of **2a** (eq 2).

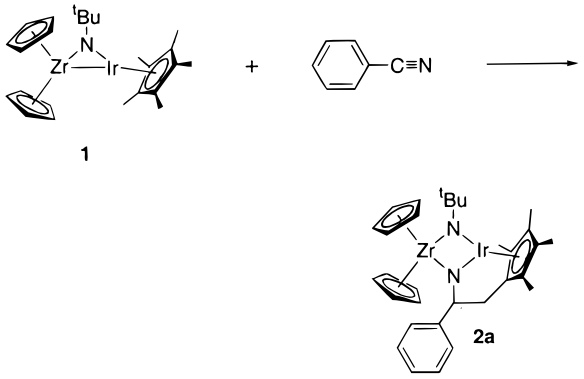

(2)

The ^{1}H NMR spectrum of **2a** exhibits two inequivalent cyclopentadienyl (Cp) ligand resonances at δ 5.42 and 5.48. Four singlets integrating to three hydrogens each are observed in the aliphatic region and three doublet of doublets, integrating to one hydrogen each, are observed at δ 2.85, 3.16, and 6.37. DEPT experiments showed the presence of a methylene carbon at 38.6 ppm, as well as a methyne carbon at 97.3 ppm in addition to the Cp methyne carbons. These data imply that a Cp* methyl group has participated in the reaction.

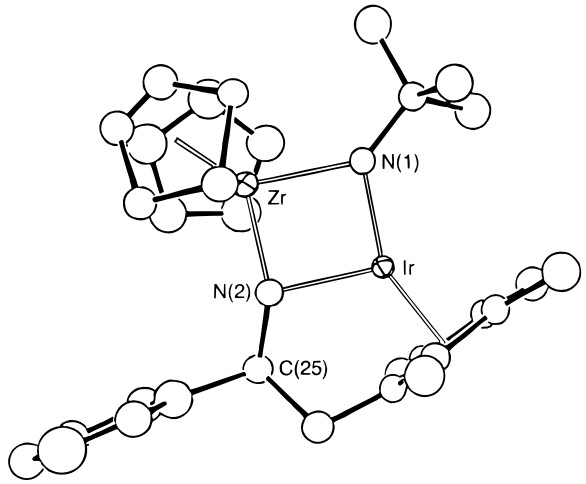

Figure 1. ORTEP diagram of $Cp_2Zr(\mu$-N-^{t}Bu)(μ-NCPhCH$_2$-η^5-C_5Me_4)Ir (**2a**). The disorder in the structure is not shown.

The structure of **2a** was determined by X-ray diffraction. The structure was solved by Patterson methods and refined via standard least-squares and Fourier techniques. An ORTEP diagram is shown in Figure 1. The presence of both enantiomers of **2a** in the unit cell caused a great deal of disorder at the benzylic carbon. Despite this disorder, the analysis clearly demonstrates the connectivity of **2a**. The structure shown is consistent with the spectral data described above, in which the methylene carbon bridges between the original nitrile carbon and Cp* ring. The $ZrIrN_2$ core in **2a** appears to be planar, but the disorder in the crystal precludes interpretation of the structure at the benzonitrile moiety.

The reaction of **1** with other arylnitriles (*o*-ethylbenzonitrile, *p*-tolunitrile, α,α,α-trifluoro-*p*-tolunitrile, and 4-methoxybenzonitrile) yields similar products (**2b**−**e**; eq 3). Blue crystals of **2b**−**e** were isolated in 61−73%

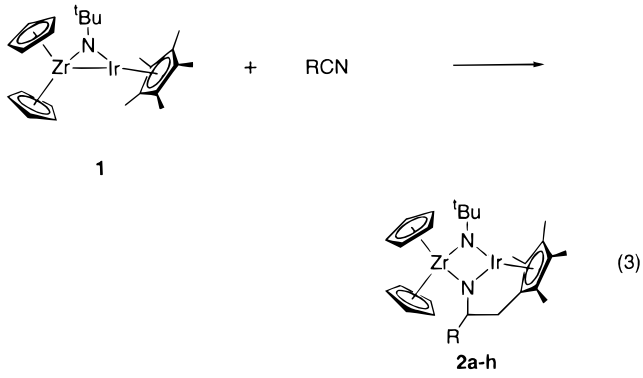

(3)

2a, R = C_6H_5
2b, R = *o*-Et-C_6H_4
2c, R = (*p*-CH_3)C_6H_4
2d, R = (*p*-CF_3)C_6H_4
2e, R = (*p*-MeO)C_6H_4
2f, R = cyclopropyl
2g, R = $CH(Me)_2$
2h, R = $NC(CH_2)_3$

yield. Analysis of the ^{1}H NMR spectra of the isolated products revealed resonances in the Cp region similar

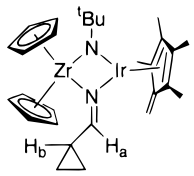

Figure 2. Proposed structure of the intermediate **3f**. Coupling is observed between H_a and H_b.

to the Cp proton resonances listed for compound **2a**. Four singlets were also observed in the alkyl region of the spectra, corresponding to the inequivalent methyl peaks on the activated Cp* ring.

Addition of Cyanoalkanes. Addition of 1 equiv of cyanocyclopropane to **1** results in the formation of the cyclometalated species $Cp_2Zr(\mu\text{-N-}^t\text{Bu})(\mu\text{-NC}(C_3H_5)(H)\text{-}CH_2\text{-}\eta^5\text{-}C_5Me_4)Ir$ (**2f**) after 8 h at room temperature. Blue crystals were isolated in 73% yield. Addition of other aliphatic nitriles (dimethylacetonitrile and 1,5-dicyanopentane) to **1** also resulted in the formation of the cyclometalated species (**2g**,**h**, respectively).

In contrast, addition of acetonitrile to **1** resulted in a red solution after 10 min. The ^{1}H NMR spectrum revealed the formation of a new Cp-containing product; however, after 1 h, multiple resonances were observed in the cyclopentadienyl region and no product was isolated. Similar observations were made when 2,2-dimethylpropionitrile, 2,2-diphenylacetonitrile, and (2-(cyanomethyl)phenyl)acetonitrile were treated with **1**.

Observation of an Intermediate in the Cyanocyclopropane Reaction. When the reaction between **1** and cyanocyclopropane was monitored by ^{1}H NMR spectroscopy in toluene-d_8, **1**, cyanocyclopropane, and two new metal-containing species were observed in the reaction mixture. We assigned one of these as the cyclometalated species **2f**. The resonances for the third compound (**3**) grow in and then subsequently disappear as the reaction proceeds to completion. This intermediate was not isolable, but analysis by NMR spectroscopy allows us to propose the connectivity shown in Figure 2. This complex has a tetramethylfulvene ligand on iridium and an alkylidene−amido moiety bridging the zirconium and iridium metal centers, resulting in a diazadimetallacyclobutane.

The ^{1}H NMR spectrum taken at 3 h reveals multiple broad resonances in the spectrum corresponding to **3**. Cooling the reaction mixture to −60 °C results in decoalescence of the resonances. Two signals are observed at δ 5.80 and 5.65 ppm, consistent with the presence of two inequivalent cyclopentadienyl ligands. The four inequivalent methyl groups of the fulvene (former Cp*) ligand on iridium are found in the aliphatic region. Resonances corresponding to the fulvene olefinic hydrogens are observed at δ 4.07 and 3.91. A doublet integrating to one hydrogen is observed at δ 7.26. We tentatively assigned this resonance to the hydrogen on the former nitrile carbon (H_a, Figure 2). Many overlapping resonances are observed in the aliphatic region, and so a total correlation spectroscopy (TOCSY) experiment was performed at −60 °C. This revealed coupling between the doublet at δ 7.26 (H_a) and a cyclopropyl hydrogen at δ 1.7 (H_b), indicating that the former nitrile carbon is indeed bound to a hydrogen.

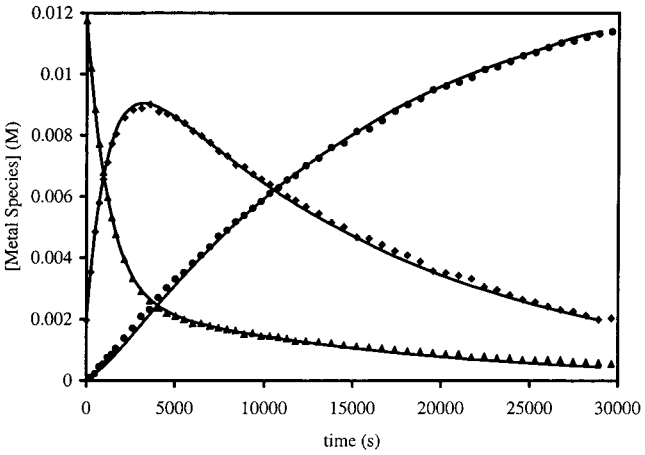

Figure 3. Representative plot of the kinetic data for the reaction of **1** with cyanocyclopropane. The curves are nonlinear regression least-squares best fits of the experimental data determined using eq 4.

Scheme 1

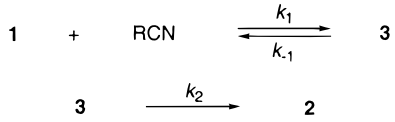

The concentrations of the starting material (**1**), intermediate **3**, and product **2f** were monitored over time by ^{1}H NMR spectroscopy at 15 °C. A representative plot of the change in concentration of the metal-containing species (**1**, **2f**, and **3**) is shown in Figure 3. To determine whether the fulvene species **3** was a productive or a nonproductive intermediate, a kinetic simulation was performed using the programs GEAR and GIT.[23−26] This provided a nonlinear regression with least-squares fitting of the experimental data.[24] We attempted to fit the data to a variety of kinetic models. Our best fit was to the model shown in Scheme 1 and eq 4.

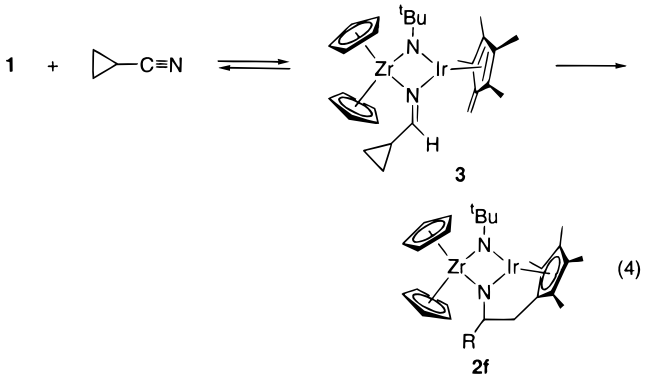

This model depicts the reversible formation of a productive intermediate, followed by irreversible prod-

(23) Espenson, J. H. *Chemical Kinetics and Reaction Mechanisms*, 2nd ed.; McGraw-Hill: New York, 1995.
(24) McKinney, R. J.; Weigert, F. J. GEAR (v. 2.1) and GIT (v. 2.1); E. I. DuPont & Nemours Co., Wilmington, DE, 1987.
(25) Krska, S. W.; Zuckerman, R. L.; Bergman, R. G. *J. Am. Chem. Soc.* **1998**, *120*, 11828.
(26) Mobley, T. A.; Schade, C.; Bergman, R. G. *Organometallics* **1998**, *17*, 3574.

Table 1. Rate Constants Produced by Nonlinear Regression Least-Squares Analysis of Experimental Data Using the Model Shown in Scheme 1

k_1	$(2.6 \pm 0.1) \times 10^{-3}$ M^{-1} s^{-1}
k_{-1}	$(1.3 \pm 0.1) \times 10^{-4}$ s^{-1}
k_2	$(7.62 \pm 0.03) \times 10^{-5}$ s^{-1}

uct formation. Figure 3 also shows the best nonlinear least-squares fits of the experimental data determined using the kinetic model in Scheme 1. Table 1 lists the rate constants calculated using this model.

The kinetic data also allowed us to calculate the equilibrium constant between the starting materials (**1** and cyanocyclopropane) and the intermediate **3** (K_{eq} = 20.6 M^{-1}). This gives $\Delta G° = -1.7$ kcal mol^{-1} for the equilibrium between the starting materials and the intermediate.

Reaction of 1 with 2-Arylacetonitriles. In contrast to the above experiments, addition of 1 equiv of phenylacetonitrile to **1** gives a mixture of two products in a 1:1 ratio after 2 days at 25 °C (eq 5). Complex **4a** is

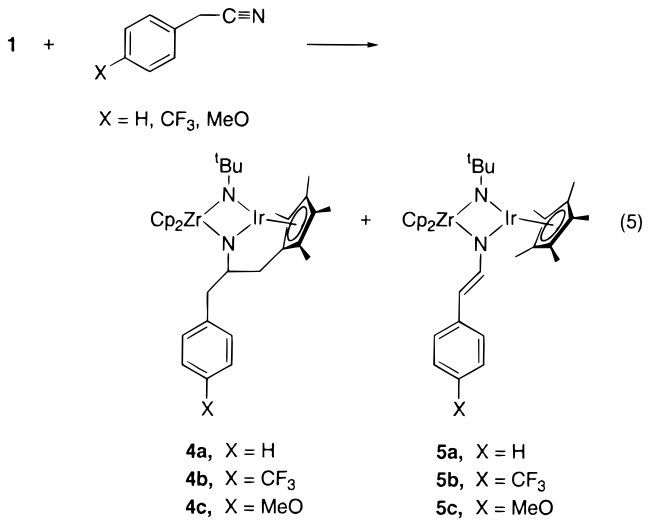

analogous to the cyclometalated species **2** previously discussed. The second product (**5a**) is a 1:1 adduct of **1** and phenylacetonitrile and is the result of insertion of the nitrile nitrogen into the zirconium−iridium bond concurrent with a 1,2-shift of a benzylic hydrogen. The two resonances corresponding to the olefinic hydrogens are observed in the ^{1}H NMR spectrum at δ 6.20 and 8.82. A single Cp resonance integrating to 10 H is observed at δ 5.88, a *tert*-butyl resonance is observed at δ 1.60, and a Cp* resonance is observed at δ 1.34.

Repeating the reaction at 45 °C and at 75 °C using 1 equiv of nitrile revealed a strong dependence of the **5a**:**4a** ratio on temperature. The observed product ratios were 1:4 and 1:20, respectively, with the cyclometalated complex **4a** as the major product in each case. There was an equally strong but opposite dependence on nitrile concentration: addition of 10 equiv (160 mM) of phenylacetonitrile to **1** at room temperature yields a product ratio of 4:1 with the olefinic complex **5a** as the major product. The same reaction at 75 °C gave a product ratio of 1:1. These data are consistent with competing bimolecular and unimolecular pathways (vide infra).

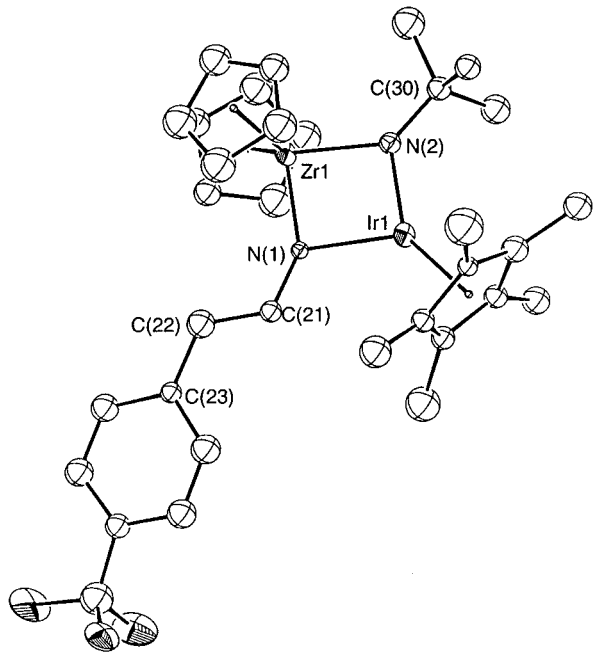

Figure 4. ORTEP diagram of $Cp_2Zr(\mu$-N-^{t}Bu)(μ-N-CHCH-(p-$CF_3C_6H_4$))IrCp* (**5b**), with atom-labeling scheme.

Control experiments showed that, after the formation of products, no change in the product ratio is observed upon heating the reaction mixture. Addition of extra phenylacetonitrile to the product mixture also has no effect on the product ratio. This demonstrates that the products **4a** and **5a** are *not* interconvertible under the reaction conditions.

The cyclometalated species **4a** was isolated in 69% yield by performing the reaction under dilute conditions for 1 day at 75 °C. The olefinic species **5a** proved to be difficult to isolate, and a maximum of 7% isolated yield was obtained. Mass spectroscopy confirmed that **5a** was a 1:1 adduct of **1** and phenylacetonitrile.

Addition of 1 equiv of (4-(trifluoromethyl)phenyl)-acetonitrile to **1** in benzene at room temperature results in the formation of a green solution after 1 h. Two products are observed by ^{1}H NMR spectroscopy in a 1:9 ratio. The ^{1}H NMR spectrum also reveals the major product (**5b**) to be analogous to the olefinic species **5a** and the minor product (**4b**) to correlate to the cyclometalated species **4a**. After multiple attempts at isolating the major product, complex **5b** was isolated in 45% yield by performing the reaction at high concentration of **1** and nitrile followed by crystallizing the product from toluene.

The olefinic species **5b** was recrystallized by slowly cooling a concentrated toluene solution of **5b** to −30 °C for 1 week. X-ray-quality crystals were obtained, and the structure of **5b** was determined by X-ray diffraction. The ORTEP diagram of **5b** is shown in Figure 4.

Selected bond lengths and bond angles are shown in Table 2, and selected crystallographic data are shown in Table 3. The bond between N1 and C21 (1.34 Å) is relatively short for a carbon−nitrogen single bond, and the bond between C21 and C22 (1.40 Å) is relatively long for a carbon−carbon double bond. C21 also lies in the plane formed by the metallacycle. These data are consistent with electron delocalization throughout the zirconium−iridium−ene−amide system.

Table 2. Selected Bond Lengths (Å) and Angles (deg) for Complex 5b

Ir1−Zr1	2.930(3)	N1−C21	1.34(3)
Ir1−N1	2.10(2)	C21−C22	1.40(3)
Ir1−N2	1.93(2)	C22−C23	1.45(3)
Zr1−N1	1.99(2)	N2−C30	1.45(3)
Zr1−N2	2.07(2)		
N1−Ir1−N2	87.3(7)	N1−C21−C22	124(2)
Ir1−N1−Zr1	91.6(7)	C21−C22−C23	123(2)
Ir1−N2−Zr1	94.1(8)	Ir1−N2−C30	130(2)
Ir1−N1−C21	122(1)	Zr1−N2−C30	136(2)
Zr1−N1−C21	146(2)	C100−Zr1−C101	126.5(1)

Table 3. Selected Crystallographic Data for Compound 5c

empirical formula	$IrZrF_3N_2C_{33}H_{35}$
fw	800.09
cryst dimens (mm)	0.43 × 0.08 × 0.01
cryst syst	orthorhombic
space group	$P2_12_12_1$
a (Å)	9.0023(2)
b (Å)	11.9204(2)
c (Å)	28.7480(3)
V (Å^3)	3084.98(8)
Z	4
ρ(calcd) (g/mol)	1.723
collecn temp (K)	−122 ± 1
F_{000}	1564.0
μ(Mo Kα) (cm^{-1})	47.01
total no. of unique rflns	2899
no. of variable params	186
R1	0.062
wR2	0.067
goodness of fit (GOF)	1.33

Addition of (4-methoxyphenyl)acetonitrile to **1** also yields two products, **4c** and **5c**. Both compounds were isolated and characterized; however, as with **5a**, only a low isolated yield of **5c** could be obtained. The product distribution is analogous to that observed in the reaction between **1** and phenylacetonitrile, with **5c** favored at higher concentrations and lower temperatures (vide infra).

Kinetic Study of the Reaction of 1 with 2-Arylacetonitriles. UV−vis and ^{1}H NMR spectroscopy were both utilized to determine the rate constant for the reaction of **1** with 2-arylnitriles. Reactions were performed under pseudo-first-order conditions using a large excess of 2-arylacetonitrile.

The reaction of **1** with (4-methoxyphenyl)acetonitrile was monitored by ^{1}H NMR spectroscopy, and observed rate constants for three (4-methoxyphenyl)acetonitrile concentrations were obtained. A typical plot of the change in concentration of the three different metal-containing species (**1**, **4c**, and **5c**) over time is shown in Figure 5.

The starting metal species **1** is observed to decay as the products **4c** and **5c** grow in. Close analysis of the spectra during the course of the reaction reveals no observable intermediate. Integration against an internal standard does show up to a 10% mass loss. The observed rate constants for the reaction of **1** with phenylacetonitrile and (4-(trifluoromethyl)phenyl)acetonitrile were measured by UV−vis spectroscopy. The correspondence between the NMR data and the UV−vis data was ascertained by monitoring the reaction of **1** plus (4-methoxyphenyl)acetonitrile by UV−vis spectroscopy and comparing the results with the data obtained using ^{1}H NMR spectroscopy. The data were found to be in good agreement. Figure 6 is a typical plot of the observed rate constants versus the concentration of 2-arylacetonitrile for the reaction of **1** plus 2-arylacetonitrile. The reaction was found to be first order in 2-arylacetonitrile, yielding a bimolecular rate law (eq 6).

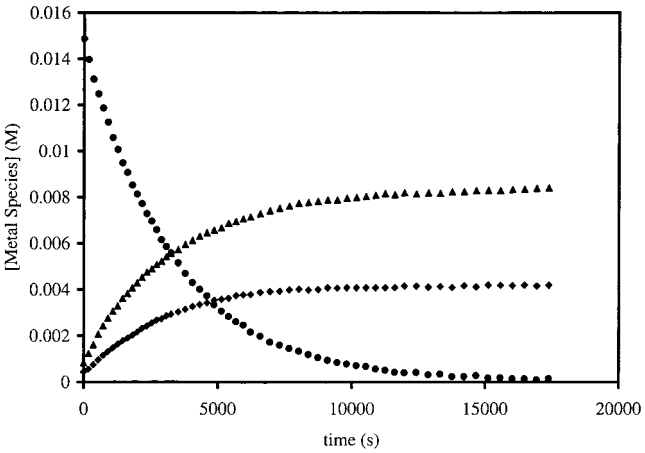

Figure 5. Disappearance of **1** (circles) and appearance of **4c** (diamonds) and **5c** (triangles) at 25 °C in C_6D_6 followed by ^{1}H NMR spectroscopy.

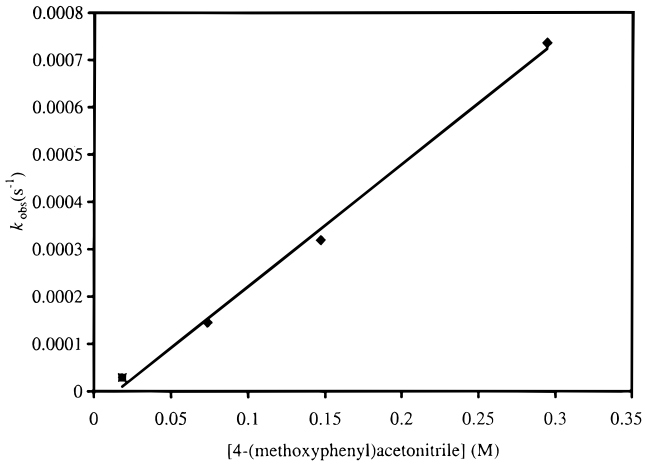

Figure 6. Plot of k_{obs} vs [**1**] (the diamonds represent the ^{1}H NMR spectroscopy data, and the square represents the UV−vis data point). This gives $k_1 = [2.6(\pm 0.1)] \times 10^{-3}$ M^{-1} s^{-1}.

Table 4. Rate Data for the Reaction of 1 with 2-Arylacetonitriles at 25 °C

nitrile	rate (M^{-1} s^{-1}) (±5%)
phenylacetonitrile	2.5×10^{-3}
phenylacetonitrile-d_2	2.1×10^{-3}
(4-(trifluoromethyl)phenyl)acetonitrile	2.3×10^{-2}
(4-(trifluoromethyl)phenyl)acetonitrile-d_2	1.7×10^{-2}
(4-methoxyphenyl)acetonitrile	2.6×10^{-3}

$$\frac{-\mathrm{d}[\mathbf{1}]}{\mathrm{d}t} = k[\mathbf{1}][\mathrm{RCN}] \qquad \mathrm{RCN} = \text{2-arylacetonitrile} \quad (6)$$

The second-order rate constants determined in this study are tabulated in Table 4. The reaction of **1** with (4-(trifluoromethyl)phenyl)acetonitrile is an order of magnitude faster than the reaction of **1** with phenylacetonitrile and also faster than that of **1** with (4-methoxyphenyl)acetonitrile.

Reaction with $PhCD_2CN$. Addition of 1 equiv of $PhCD_2CN$ to **1** gave the expected products (**4a-*d*$_2$** and **5a-*d*$_2$**; eq 7). However, a product ratio of 1:20 for **5a-*d*$_2$**:**4a-*d*$_2$** is observed at 25 °C and 16 mM $PhCD_2CN$. Analysis by ^{1}H NMR and ^{2}H NMR spectroscopy revealed quantitative deuterium incorporation into the benzylic positions of complex **4a**. The ^{1}H NMR spectrum of **5a-*d*$_2$** shows a singlet at δ 8.82 in place of the doublet for the vinyl hydrogen located α to the metallacycle in the protiated analogue of **5a**.

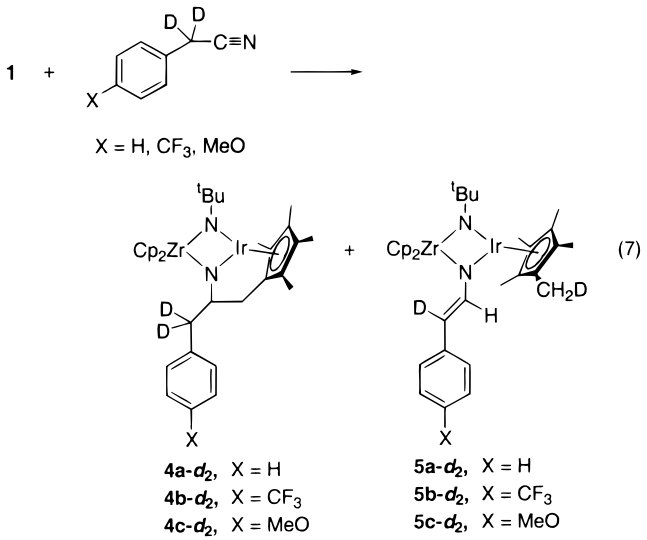

No resonance is observed at δ 6.20 in the ^{1}H NMR spectrum, but a resonance is observed at δ 6.20 in the ^{2}H NMR spectrum. We conclude that **5a-*d*$_2$** has a deuterium bound to the carbon α to the phenyl ring and a hydrogen bound to the carbon α to the metallacycle. A second resonance is observed at δ 1.34 ppm in the ^{2}H NMR spectrum, indicating that the second deuterium is incorporated into the Cp* ring of **5a** (eq 7).

Labeled 4-(methoxyphenyl)acetonitrile and (4-(trifluoromethyl)phenyl)acetonitrile reacted individually with **1** to give **4b-*d*$_2$**, **5b-*d*$_2$**, **4c-*d*$_2$**, and **5c-*d*$_2$**, respectively. Deuterium incorporation is observed in the analogous positions of **4a-*d*$_2$** and **5a-*d*$_2$**.

Attempts at crossover experiments led to inconclusive results. When $PhCD_2CN$ and 4-(methoxyphenyl)acetonitrile were combined in solution and heated to 75 °C, no hydrogen−deuterium exchange was observed after 2 days. However, when a solution containing 8.2 mM $PhCD_2CN$, 6.2 mM 4-(methoxyphenyl)acetonitrile, and 16 mM **1** was prepared, deuterium scrambling was observed in both the products and the nitriles (eq 8).

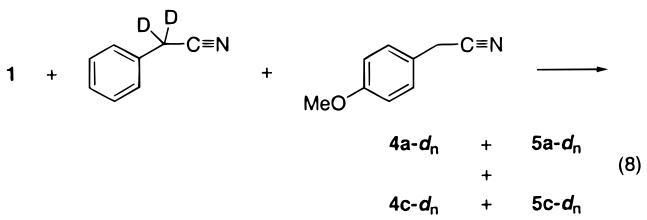

Thus, **1**, or products formed from **1** and the 2-arylacetonitriles, apparently catalyzes deuterium exchange between the α-positions of the nitriles. These reactions were carried out in silylated NMR tubes to prevent catalytic hydrogen/deuterium scrambling by the hydroxyl groups on the glassware.

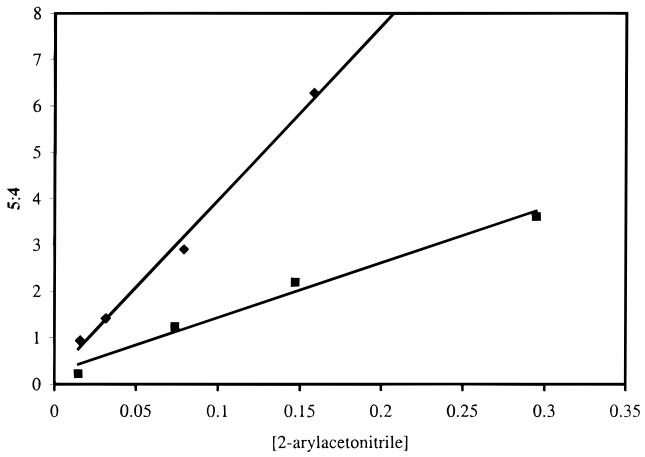

Figure 7. Plot of the **5**:**4** ratio vs the concentration of 2-arylacetonitrile. The diamonds represent the **5a**:**4a** product ratio, and the squares represent the **5c**:**4c** product ratio.

Dependence of Product Ratio on the Concentration of 2-Arylacetonitrile. A particularly unusual aspect of this reaction is the dependence of the product ratio on the initial concentration of nitrile. A plot of the product ratio (ratio of the olefinic species **5a** to the cyclometalated species **4a**) vs the phenylacetonitrile concentration is shown in Figure 7. The plot reveals an approximately linear correlation between the concentration of phenylacetonitrile and the product ratio, indicating that the reaction order in nitrile for the formation of **5a** is one unit higher than the reaction order in nitrile for the formation of **4a** (eq 9).[23]

$$\frac{\mathrm{d}[\mathbf{5}]/\mathrm{d}t}{\mathrm{d}[\mathbf{4}]/\mathrm{d}t} = \frac{k_5[\mathbf{1}][\mathrm{RCN}]^Y}{k_4[\mathbf{1}][\mathrm{RCN}]^X} = \frac{[\mathbf{5}]_\infty}{[\mathbf{4}]_\infty} \qquad Y = X + 1 \quad (9)$$

The above experiment was repeated for the reaction of **1** and (4-methoxyphenyl)acetonitrile (Figure 7). A linear dependence of the **5c**:**4c** ratio on the concentration of (4-methoxyphenyl)acetonitrile is observed, supporting the relationship shown in eq 9 for this system.

The olefinic species **5b** is strongly favored in the reaction of **1** with (4-(trifluoromethyl)phenyl)acetonitrile, even at low concentrations (16 mM) of nitrile and complex **1**. Addition of (4-(trifluoromethyl)phenyl)acetonitrile to the reaction mixture of **1** and (4-methoxyphenyl)acetonitrile results in four different products: **4b**, **4c**, **5b**, and **5c**. The *methoxy* product ratio **5c**:**4c** is greatly enhanced by the addition of the *fluorinated* nitrile. Varying the initial concentration of (4-(trifluoromethyl)phenyl)acetonitrile while keeping the initial concentration of **1** and (4-methoxyphenyl)acetonitrile constant resulted in a linear dependence of the product ratio **5c**:**4c** (the products derived from the reaction of **1** with (4-methoxyphenyl)acetonitrile) on the concentration of (4-(trifluoromethyl)phenyl)acetonitrile (Figure 8).

This concentration dependence was observed in experiments in which less than 1 equiv of (4-(trifluoromethyl)phenyl)acetonitrile was used. This occurred even though the reaction of **1** with (4-(trifluoromethyl)-phenyl)acetonitrile is an order of magnitude faster than the reaction of **1** with (4-methoxyphenyl)acetonitrile. It is important to note that because the fluorinated nitrile

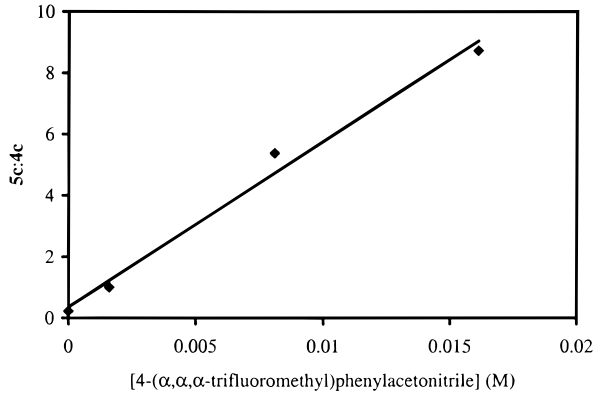

Figure 8. Plot of the **5c**:**4c** product ratio vs the concentration of (4-(trifluoromethyl)phenyl)acetonitrile.

Table 5. List of Added Substrates and Their Effect on the Product Distribution (5c:4c)

substrate	effect
triethylamine	none
pyridine	none
Proton Sponge (1,8-bis(dimethylamino)-naphthalene)	none
cyanocyclopropane	none
potassium cyanide	none
indene	none
9-phenylfluorene	very small increase
hexafluorobenzene	none
1,4-bis(trifluoromethyl)benzene	none
tris(dimethylamino)sulfur (trimethylsilyl)difluoride (TAS-F, catalytic amount)	none
methyl phenylacetate	none
methyl 4-(trifluoromethyl)benzoate	none
4-(trifluoromethyl)phenyl acetate	signif increase
(4-(trifluoromethyl)phenyl)acetonitrile	signif increase
(4-(trifluoromethyl)phenyl)acetonitrile-d_2	signif increase
(4-methoxyphenyl)acetonitrile	control
complex **4b**	none
reaction product mixture: **1** + (4-(trifluoromethyl)phenyl)acetonitrile	signif increase

reacts so rapidly with **1**, this nitrile has been largely converted to products **4b** and **5b** before much of the methoxy-substituted nitrile has had time to react. Therefore, it is not possible to tell from these data whether the change in methoxy-substituted product ratio **5c**:**4c** is caused by fluorinated nitrile, products formed from this nitrile, or both. We have plotted the product ratio vs the total initial concentration of added fluorinated nitrile.

A complementary experiment was performed in which the initial concentrations of **1** and (4-(trifluoromethyl)-phenyl)acetonitrile were kept constant and the concentration of (4-methoxyphenyl)acetonitrile was varied. Again, four different products were observed (**4b**, **4c**, **5b**, and **5c**). In this case the product ratio **5b**:**4b** (the products derived from the reaction of **1** with (4-(trifluoromethyl)phenyl)acetonitrile) did *not* depend on the concentration of (4-methoxyphenyl)acetonitrile.

In an attempt to determine what other types of additives might influence the **5c**:**4c** product ratio, a variety of different substrates, listed in Table 5, were added to a mixture of **1** and (4-methoxyphenyl)acetonitrile. The initial concentrations of **1** and (4-methoxyphenyl)acetonitrile were kept at 16 mM each as the concentration of added substrate was varied. These substrates can be classified into five separate categories: bases,

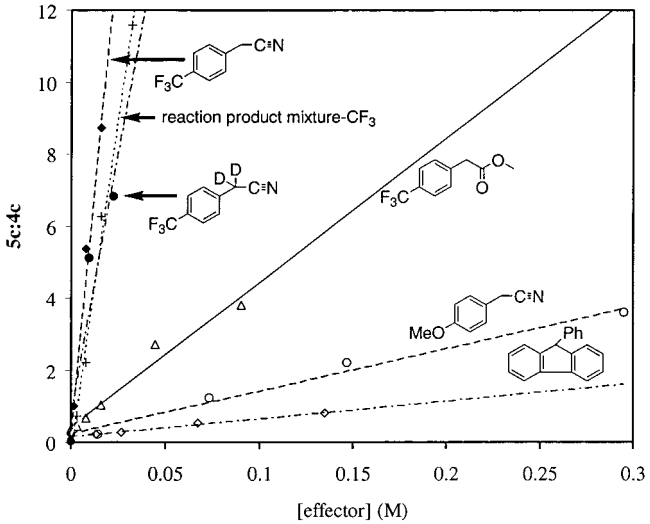

Figure 9. Plot of the **5c**:**4c** product ratio vs the effector concentration.

carbon acids, fluorinated compounds including a fluoride source, esters, and compounds in the reaction mixture. This fifth class includes the purified fluorinated products **5b** and also the final reaction mixture of **1** and (4-(trifluoromethyl)phenyl)acetonitrile. None of the compounds in the first four groups react with or destroy the starting materials at an appreciable rate except for TAS-F. In this case, only a catalytic amount of substrate was used. A few of these additives did enhance the **5c**:**4c** product ratio. These substrates will be referred to as "effectors", since they have the ability to modify the product ratio in the reaction of **1** with 2-arylacetonitriles. Figure 9 shows the effect some of these compounds have on the **5c**:**4c** product ratio. The ratios all change linearly, but with strongly different slopes.

Three noteworthy results were observed with the fifth class of compounds. First, the reaction product mixture of **1** and (4-(trifluoromethyl)phenyl)acetonitrile influenced the product distribution **5c**:**4c** as much as (4-(trifluoromethyl)phenyl)acetonitrile itself (within error). Second, no significant isotope effect was observed when deuterated (4-(trifluoromethyl)phenyl)acetonitrile was used as the effector. Third, the purified trifluoromethyl-substituted product **5b** did not enhance the product distribution.

Discussion

Reaction of 1 with Cyanoarenes and Cyanoalkanes. The reaction between **1** and several cyanoarenes and cyanoalkanes results in the formation of cyclometalated species **2a**−**h**. These reactions proceed cleanly and quantitatively by ^{1}H NMR spectroscopy. The formation of these cyclometalated species involves hydrogen transfer from a Cp* methyl group to the electrophilic carbon center of the nitrile.

For this reaction, the simplest mechanism we can envision that is consistent with our data is illustrated in Scheme 2. The nitrile first attacks the Zr−Ir bond, perhaps giving a side-on bound complex (**6**) analogous to that observed with CO_2 (eq 1). Tilley and co-workers observed similar side-on-bound cyano complexes in their

Scheme 2

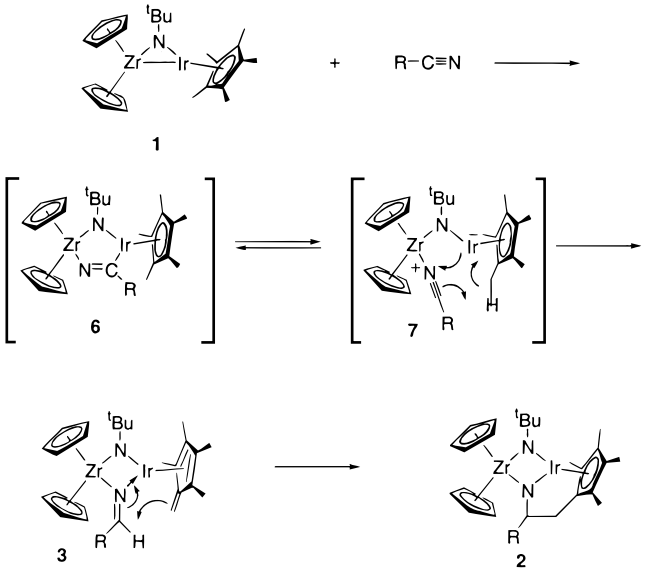

Zr−Si systems.[27] Complex **6** could be in equilibrium with a zwitterionic terminally bound species **7**, in which the nitrile is activated by coordination of its nitrogen atom to the electropositive Zr center. Proton transfer from one of the Cp* methyls to the nitrile carbon leads to the (observable) fulvene complex **3**, and this is followed by attack of the fulvene methylene group at the alkylidene−amido ligand to give the final cyclometalated product **2**.

Intermediate **3** possesses a fulvene ligand on the iridium metal center and a bridging alkylidene−amido moiety. Iridium fulvene complexes have been reported to have many different binding modes.[28−33] The chemical shift of the methylene hydrogens is most consistent with an η^4-binding mode as opposed to an η^6-binding mode,[31] but this is only speculative, since the material was too reactive to isolate and characterize by X-ray diffraction. The broadness of the resonances in the ^{1}H NMR spectrum at room temperature is consistent with rapid rotation of the fulvene around the metal−ligand axis. Similar behavior has been observed by our group in another iridium η^4 fulvene complex.[32] At −60 °C, the rotation is slow enough to freeze out the spectrum of the most stable rotamer of complex **3**. This is seen most clearly by the presence of four different methyl resonances and two different Cp resonances in this species.

The metal centers in **3** form a diazametallacyclobutane complex with two nitrogens at opposing corners of the ring. One of the nitrogens is derived from the original *tert*-butylimido bridge, while the other is part of a bridging alkylidene amido ligand. Similar bridging alkylidene amido complexes have been observed in a few other bimetallic,[14,18,34,35] including heterobimetallic,[14,18] complexes.

No intermediate is observed in the reaction of **1** with cyanoarenes. This can be attributed to a low barrier for isomerization of the intermediate (**3**) to the product (**2**).

Reaction of 1 with 2-Arylacetonitriles. Addition of 2-arylacetonitriles to **1** results in the formation of two noninterconvertible products, **4** and **5** (eq 5). Product **4** is analogous to the complex formed in the reaction of **1** with cyanoarenes and several cyanoalkanes. We assume it is formed through a pathway similar to that for **2**. However, as is the case with cyanoarenes, no intermediate is observed.

The mechanism of formation of olefinic product **5** is less clear, as are the causes of the increase in yield of this product produced by lowering the temperature or increasing the concentration of 2-arylacetonitrile. One fundamental mechanistic question is whether the two products **4** and **5** are formed in completely independent pathways (eq 10) or in a branching mechanism. In the

$$\mathbf{1} + \mathrm{RCN} \xrightarrow{k_4} \mathbf{4}$$

$$\mathbf{1} + \mathrm{RCN} \xrightarrow{k_5} \xrightarrow{\mathrm{RCN}} \mathbf{5} \qquad (10)$$

latter process **1** would react with the nitrile to form an intermediate that then could be converted to either **4** or **5**, depending on the intermediate structure or the reaction conditions (eq 11).

$$\mathbf{1} + \mathrm{RCN} \xrightarrow{k_3} \mathbf{3} \begin{cases} \xrightarrow{k_4} \mathbf{4} \\ \xrightarrow{k_5[\mathrm{RCN}]} \mathbf{5} \end{cases} \qquad (11)$$

Kinetic, product ratio dependence, isotope tracer, and kinetic isotope effect data support the branching mechanism, with the heterodinuclear fulvene complex **3** postulated in Scheme 3 as the branching point. In this scenario complex **4** is formed from **3** as discussed earlier (Scheme 2), and conversion of **3** to **5** occurs by transfer of a hydrogen atom from the benzylic carbon to the fulvene methylene carbon in **3**, regenerating the C_5Me_5 group as **5** is formed. In agreement with this mechanism, deuterium is found in one vinyl position of **5** and in its Cp* ring (eq 7).

Monitoring the rate of disappearance of **1** established an overall second-order rate law for the disappearance of starting materials (eq 6). This rate law is consistent with either the branching or parallel path mechanisms. However, the isotope effects (k_H/k_D) observed upon replacement of the benzylic hydrogens in the nitrile reactant with deuterium atoms are small, considering that they involve C−H (C−D) bond cleavage: 1.19 for the reaction of **1** with phenylacetonitrile and 1.35 for the reaction of **1** with (4-(trifluoromethyl)phenyl)acetonitrile. In view of the low magnitude of these effects it seems unlikely that benzylic C−H bond cleavage occurs in, or prior to, the rate-determining transition state for formation of either product. This is consistent with the mechanism outlined in Schemes 2 and 3.

(27) Woo, H. G.; Tilley, T. D. *J. Organomet. Chem.* **1990**, *393*, C6.
(28) Kolle, U.; Kang, B.; Thewalt, U. *J. Organomet. Chem* **1990**, *386*, 267.
(29) Mach, K.; Varga, V.; Hanus, V. *J. Organomet. Chem.* **1991**, *415*, 87.
(30) Klahn, A. H.; Oelckers, B.; Godoy, F.; Garland, M. T.; Vega, A.; Perutz, R. N.; Higgitt, C. L. *J. Chem. Soc., Dalton Trans.* **1998**, 3079.
(31) Parkin, G.; Bercaw, J. E. *Polyhedron* **1988**, *7*, 2053.
(32) Glueck, D. S.; Bergman, R. G. *Organometallics* **1990**, *9*, 2862−2863.
(33) Schock, L. E.; Brock, C. P.; Marks, T. J. *Organometallics* **1987**, *6*, 232.
(34) Evans, W. J.; Meadows, J. H.; Hunter, W. E.; Atwood, J. L. *J. Am. Chem. Soc.* **1984**, *106*, 1291.
(35) Klose, A.; Solari, E.; Floriani, C.; Chiesi-Villa, A.; Rizzoli, C.; Re, N. *J. Am. Chem. Soc.* **1994**, *116*, 9123.

Scheme 3

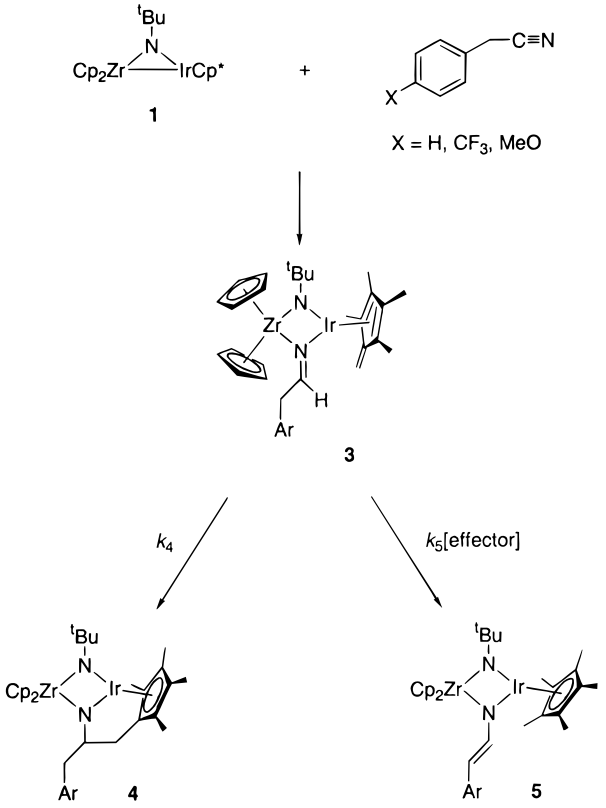

The strongest evidence for the branching mechanism comes from the dependence of the **5**:**4** product ratio upon the concentration of starting materials. As noted earlier, the product ratio (**5**:**4**) depends linearly upon the concentration of 2-arylacetonitrile (eq 12). The linear

$$\frac{[\mathbf{5}]_\infty}{[\mathbf{4}]_\infty} = \frac{k_5[\mathbf{1}][\mathrm{RCN}]^Y}{k_4[\mathbf{1}][\mathrm{RCN}]^X} \qquad (12)$$

dependence implies that the reaction order in nitrile concentration for the formation of **5** (Y) is one unit higher than for the formation of **4** (X; eq 13). As stated

$$Y = X + 1 \qquad (13)$$

above, the rate of disappearance of complex **1** has a first-order nitrile concentration dependence. Thus, branching to the two products (**4** and **5**) must occur after the rate-determining step. In other words, the observed concentration dependence of the product distribution is a function of the partitioning of the intermediate formed in the rate-determining step.

Kinetic modeling of the reaction of **1** with cyanocyclopropane revealed that the transformation of **3** to **2** is a unimolecular process. From this, we can extrapolate that the formation of the cyclometalated species (**4**) from the intermediate is also a unimolecular process and therefore is zero order in nitrile ($X = 0$). Solving eq 12 and 14 for $X = 0$ yields eq 14.

$$\frac{[\mathbf{5}]_\infty}{[\mathbf{4}]_\infty} = \frac{k_5[\mathrm{RCN}]}{k_4} \qquad (14)$$

Role Played by the Second Molecule of Nitrile (and Certain Other "Effectors") in the Formation of Product 5. Our kinetic results indicate that a second molecule of nitrile catalyzes the conversion of intermediate **3** to product **5**. However, we frankly do not understand the nature of the role played by the nitrile in this transformation. The situation is clearly more complicated than it would be if a given nitrile only facilitated its own conversion to **5**. On the contrary, the following facts are clear.

(a) One nitrile can catalyze changes in the product distribution from another. This is demonstrated by addition of (4-(trifluoromethyl)phenyl)acetonitrile to the reaction of **1** with 4-(methoxyphenyl)acetonitrile. The methoxy product ratio **5c**:**4c** was strongly enhanced by the addition of the fluorinated nitrile. Thus, the fluorinated nitrile (or something formed from it; see (b)) is a catalyst for the conversion of the fulvene intermediate **3c** to the methoxy product **5c**.

(b) The behavior summarized in (a) occurs even though the fluorinated nitrile reacts with **1** faster than the methoxy-substituted nitrile does. The product distribution of **5c**:**4c** is also strongly enhanced by the unpurified reaction mixture formed from **1** and (4-(trifluoromethyl)phenyl)acetonitrile, and no significant isotope effect was observed on the product distribution when deuterated (4-(trifluoromethyl)phenyl)acetonitrile was used. Thus, it is possible that the formation of methoxy product **5c** is catalyzed not by the fluorinated nitrile but by something formed from the fluorinated nitrile and **1**.[36] No change in product distribution was observed upon addition of potassium cyanide or TAS-F, a fluoride source.

(c) A trend was observed in the product ratio dependence upon the pK_a value of the benzylic hydrogens of the nitrile. The more acidic nitriles (i.e., (4-(trifluoromethyl)phenyl)acetonitrile) tended to form a higher proportion of the olefinic complex **5**, and the less acidic nitriles (i.e., 4-(methoxyphenyl)acetonitrile) tended to form a higher proportion of the cyclometalated complex **4**. We considered the possibility that this property was important in the catalyst and examined other weak carbon acids as effectors. Only one (9-phenylfluorene) was found to influence the **5**:**4** product distribution, and the effect was very small. Attempts at investigating stronger acids were unsuccessful due to the reactivity of the acids toward **1**. Addition of compounds with aryl or benzylic fluorine atoms (hexafluorobenzene, 1,4-bis-(trifluoromethyl)benzene) did not change the product distribution.

(d) The only non-nitrilic compound found to strongly affect the **5**:**4** product ratio was 4-(trifluoromethyl)-phenyl acetate. The benzylic hydrogens and fluorinated substituent are apparently required for this result, since no enhancement was observed upon addition of methyl phenylacetate or methyl 4-(trifluoromethyl)benzoate.

Clearly an unusual phenomenon is at work here,[37−39] and further studies will be required to determine its cause.

(36) A linear relationship between the product distribution **5**:**4** and 2-arylacetonitrile concentration is still possible if an impurity catalyzes the formation of **5**.

(37) The role of the "effector" is similar to Wulff's "allochemical effect", in which a second molecule of substrate influences the product distribution but is not involved in the stoichiometry of the reaction.[38,39]

(38) Bos, M. E.; Wulff, W. D.; Miller, R. A.; Chamberlin, S.; Brandvold, T. A. *J. Am. Chem. Soc.* **1991**, *113*, 9293.

(39) Waters, M. L.; Bos, M. E.; Wulff, W. D. *J. Am. Chem. Soc.* **1999**, *121*, 6403.

Conclusion

In this study we have found that the Zr−Ir bond in heterobimetallic complex **1** is reactive toward nitriles, leading to overall products in which the C−N bond multiplicity has been reduced from 3 to 1 and the nitrile nitrogen forms an amido bridge between the two metal centers. The specific products formed depend on the type of nitrile used in the reaction. Addition of simple cyanoalkanes and -arenes to complex **1** result in the formation of cyclometalated species **2**, in which a new C−C bond is formed and a hydrogen has been transferred from the Cp* ligand to the cyano carbon. With arylacetonitriles, a cyclometalated product **4** analogous to **2** is observed, but this is accompanied by variable amounts of a second (olefinic) product **5**, in which a net 1,2-shift of the benzylic hydrogen to the former nitrile carbon has occurred.

Kinetics, isotope labeling, and product distribution studies have provided substantial information about the mechanism of this reaction. The route leading to the cyclometalated product, outlined in Schemes 2 and 3, is relatively well understood and proceeds via the (in some cases detectable) fulvene intermediates **3**, which undergoes unimolecular conversion to **2** and **4**. Compound **5** is also formed from this intermediate, but in this case a second molecule or "effector" is involved in this pathway. This reaction therefore has the unusual characteristic that an organic compound is the apparent catalyst for an organometallic transformation. Such observations are rare, but a similar effect has been reported (albeit in a chemically different system) by Wulff and co-workers; they have termed this the "allochemical effect."[37−39]

An initial investigation indicated that a second molecule of arylacetonitrile can serve as an effector. However, nitriles other than the one that initially reacts, as well as certain specific other molecules, can serve as effectors. The lack of a clear pattern among the molecules that serve as effectors, and those that do not, has frustrated our efforts to determine the detailed mechanism by which **3** is converted to **5**. Thus, an observation which initially seemed rather simple (that the conversion of **3** to **5** was catalyzed by a second molecule of starting nitrile) was revealed to be substantially more complicated than it appeared at first, and further study will be required to sort out the perplexing mechanistic questions raised by these results.

Experimental Section

General Comments. All manipulations were carried out under an inert atmosphere or by using standard Schlenk or vacuum line techniques unless noted otherwise. The ^{1}H and ^{13}C NMR spectra were obtained on Bruker 300 and 400 MHz Fourier transform spectrometers with commercial Bruker AMX series interfaces or a Bruker 500 MHz Fourier transform spectrometer with a commercial Bruker DRX series interface. All *J* values are given in Hz.

$Cp_2Zr(\mu$-N-^{t}Bu)IrCp* (**1**) was prepared by literature methods.[4] All other reagents were purchased from commercial vendors, checked for purity, and used without further purification unless otherwise noted. Liquids were degassed using three freeze−pump−thaw cycles. Liquid reagents were dried over 4 Å activated molecular sieves or passed through an activated alumina column. Phenylacetonitrile and (4-methoxyphenyl)-acetonitrile were distilled under reduced pressure and passed through an activated alumina column. Solids were stored in an inert-atmosphere box. Benzene, pentane, and hexanes (UV grade, alkene free) were either distilled from purple sodium/benzophenone ketyl under nitrogen or passed through a column of activated alumina (A1, 12 × 32, Purifry) under nitrogen pressure and sparged with nitrogen prior to use. Toluene was either distilled from sodium metal or passed through a column of activated alumina (A1, 12 × 32, Purifry) under nitrogen pressure and sparged with nitrogen prior to use. Diethyl ether and tetrahydrofuran were distilled from purple sodium/benzophenone ketyl under nitrogen. The deuterated solvents used in NMR experiments were either vacuum-transferred from sodium/benzophenone ketyl and stored under inert atmosphere or degassed by three freeze−pump−thaw cycles, placed over 4 Å activated molecular sieves, and filtered through glass-fiber filter paper prior to use.

In the kinetic studies, either volumetric glassware or calibrated syringes were utilized. The error involved is estimated to be less than 5%.

$Cp_2Zr(\mu$-N-^{t}Bu)(μ-NCPhCH$_2$-η^5-C$_5$Me$_4$)Ir (2a). $Cp_2Zr(\mu$-N-^{t}Bu)IrCp* (**1**; 96 mg, 1.55×10^{-4} mol) was dissolved in 13 mL of toluene. To this dark brown solution was added 15.9 μL (1.55×10^{-4} mol) of benzonitrile dissolved in 2 mL of toluene. The solution was left at room temperature for 4 days, over which time it turned dark green. It was then filtered through a medium-porosity frit to remove a small amount of unidentified brown precipitate. The solution was concentrated under reduced pressure to 2 mL and cooled to −30 °C to produce dark green crystals of **2a** (58.6 mg, 3.12×10^{-5} mol, 38%). ^{1}H NMR (THF-d_8): δ 7.73 (m, 2H), 7.45 (t, J = 5.65, 2H), 7.31 (t, J = 7.36, 1H), 6.37 (d of d, J = 5.45, 10.52, 1H), 5.48 (s, 5H), 5.42 (s, 5H), 3.16 (d of d, J = 13.76, 10.56, 1H), 2.85 (d of d, J = 5.47, 13.78, 1H), 2.00 (s, 3H), 1.93 (s, 3H), 1.91 (s, 3H), 1.86 (s, 3H), 1.59 (s, 9H). ^{13}C{^{1}H} NMR (THF-d_8): δ 149.7, 128.8, 128.5, 127.5, 108.4, 107.7, 101.1, 97.3, 94.3, 92.3, 82.4, 81.8, 70.1, 38.6, 35.3, 12.3, 11.9, 11.0, 10.6. IR (Nujol): 3096, 3028, 3001, 2926, 2803, 2776, 1495, 1441, 1345, 1284, 1195, 1100, 1025, 916, 773 cm^{-1}. Anal. Calcd for $C_{31}H_{39}IrN_2Zr$: C, 51.49; H, 5.44, N, 3.87. Found: C, 51.15; H, 5.37; N, 3.64.

X-ray Structure Determination of Complex 2a. A clump of thin stacked plates was obtained by slow cooling of a saturated toluene solution from 67 to −30 °C. One was mounted on a glass fiber using Paratone N hydrocarbon oil. It was cooled to −126 °C by a nitrogen-flow low-temperature apparatus which had been previously calibrated by a thermocouple placed at the sample position. Crystal quality was evaluated via measurement of intensities and inspection of peak scans. Automatic peak search and indexing procedures yielded an orthorhombic reduced primitive cell. Inspection of the Niggli values revealed no conventional cell of higher symmetry. The final cell parameters and specific data collection parameters for this data set are given in the Supporting Information.

The 3737 raw intensity data were converted to structure factor amplitudes and their esd's by correction for scan speed, background, and Lorentz and polarization effects. No correction for crystal decomposition was necessary. Inspection of the azimuthal scan data showed the variation $I_{min}/I_{max} = 2.09$ for the average curve. An empirical correction was made to the data based on the azimuthal scan data ($T_{max} = 0.099$, $T_{min} = 0.477$). Inspection of the systematic absences indicated space group $P2_1/n$. Removal of systematically absent data left 3639 unique data in the final data set. Hydrogen atoms were not included in structure factor calculations.

The final residuals for 191 variables refined against the 2912 accepted data for which $F^2 > 3\sigma(F^2)$ were $R = 4.0\%$, $R_w = 4.8\%$, and GOF = 1.97. The R value for all 3737 data was 5.4%. The largest peak in the final difference Fourier map had an electron density of 1.53 e/Å^3 and the lowest excursion −0.29

e/Å^3. The positional and anisotropic thermal parameters are given in the Supporting Information.

$Cp_2Zr(\mu$-N-^{t}Bu)(μ-NC(*o*-$(C_2H_5)C_6H_4)HCH_2$-η^5-$C_5Me_4)Ir$ (2b). In the drybox, 83.5 mg (1.35×10^{-5} mol) of $Cp_2Zr(\mu$-N-^{t}Bu)IrCp* was dissolved in 10 mL of toluene in a vial containing a magnetic stir bar. *o*-Ethylbenzonitrile (10 μL, 7.73×10^{-5} mol) was added via syringe. The solution was stirred for 5 min and allowed to stand overnight. The resulting solution was a dark bluish green color. The volatile materials were removed at room temperature in vacuo. The solids were redissolved in 2 mL of toluene, and 20 mL of pentane was layered onto the toluene solution. The vial was cooled to −30 °C for 3 days. Blue crystals were isolated in 63% yield (63.7 mg, 8.48×10^{-5} mol). ^{1}H NMR (C_6D_6): δ 8.27 (m, 1), 7.49 (t, 1, $J = 5.13$), 7.26 (t, 1, $J = 5.67$), 7.2 (m, 1), 6.66 (m, 1), 5.85 (s, 5), 5.58 (s, 5), 2.10 (dd, 1, $J = 14.33, 7.48$), 2.91 (m, 2), 2.68 (dd, 1, $J = 13.88, 5.20$), 1.64 (s, 9), 1.63 (s, 3), 1.56 (s, 3), 1.53 (s, 3), 1.48 (s, 3), 1.31 (t, 3, $J = 7.60$). ^{13}C{^{1}H} NMR (C_6D_6): δ 144.1, 130.7, 128.2, 127.8, 126.7, 108.4, 107.7, 100.6, 92.8, 91.8, 81.3, 81.0, 80.1, 69.7, 38.2, 35.0, 27.8, 20.7, 12.0, 11.6, 10.6, 10.4. IR (Nujol): 1456, 1376, 1349, 1018, 767 cm^{-1}. Anal. Calcd for $C_{33}H_{43}N_2ZrIr$: C, 52.77; H, 5.77; N, 3.73. Found: C, 52.68; H, 5.74; N, 3.70.

$Cp_2Zr(\mu$-N-^{t}Bu)(μ-NCH(*p*-$(CH_3)C_6H_4)CH_2$-η^5-$C_5Me_4)Ir$ (2c). A solution of $Cp_2Zr(\mu$-N-^{t}Bu)IrCp* (63.2 mg, 1.02×10^{-4} mol) and *p*-tolunitrile (12.2 μL, 1.02×10^{-4} mol) was prepared in 8 mL of toluene. The solution turned to an aquamarine color after 2 h. The volatile materials were removed under reduced pressure, and the resulting solid was crystallized from 6 mL of a 1:1 pentane−toluene mixture at −30 °C. A total of 50.1 mg (6.80×10^{-4} mol, 61%) of blue crystals was obtained. ^{1}H NMR (C_6D_6): δ 7.68 (d, 2, $J = 7.95$), 7.25 (d, 2, $J = 7.95$), 6.34 (dd, 1, $J = 10.3$, $J = 5.3$), 5.78 (s, 5), 5.66 (s, 5H), 3.06 (dd, 1, $J = 13.8$, $J = 10.5$), 2.26 (s, 3), 1.63 (s, 9), 1.62 (s, 3), 1.55 (s, 3), 1.53 (s, 3), 1.50 (s, 3). ^{13}C{^{1}H} NMR (C_6D_6): δ 147.2, 137.5, 129.3, 109.5, 107.5, 100.2, 96.9, 93.8, 92.0, 82.1, 80.4, 69.7, 38.4, 34.8, 21.2,12.4, 11.8, 10.6, 10.2. Anal. Calcd for $C_{32}H_{41}N_2ZrIr$: C, 52.14; H, 5.61; N, 3.80. Found: C, 52.16; H, 5.75; N, 3.79.

$Cp_2Zr(\mu$-N-^{t}Bu)(μ-NCH(*p*-$(CF_3)C_6H_4)CH_2$-η^5-$C_5Me_4)Ir$ (2d). The procedure used to prepare **2c** was followed, using 57.6 mg (9.29×10^{-5} mol) of $Cp_2Zr(\mu$-N-^{t}Bu)IrCp* and 15.7 mg (9.17×10^{-5} mol) of 4-(trifluoromethyl)benzonitrile in 8 mL of toluene. The solution turned to a greenish blue color after 20 min. The volatile materials were removed under reduced pressure, and the resulting solid was crystallized from 4 mL of a 1:1 pentane−toluene mixture. Blue crystals were obtained in 67% yield (49.1 mg, 6.20×10^{-5} mol). ^{1}H NMR (C_6D_6): δ 7.61 (m, 4), 6.22 (dd, 1, $J = 5.4$, $J = 11.1$), 5.70 (s, 5), 5.55 (s, 5), 2.81 (dd, 1, $J = 10.5$, $J = 13.8$), 2.52 (dd, 1, $J = 5.5$, $J = 13.8$), 1.62 (s, 3), 1.60 (s, 9), 1.53 (s, 3H), 1.49 (s, 3), 1.48 (s, 3). ^{13}C{^{1}H} NMR (C_6D_6): δ 152.5, 125.6, 108.3, 107.6, 100.4, 96.0, 93.0, 91.7, 81.3, 80.7, 69.7, 38.3, 34.9, 12.0, 11.8, 10.2, 9.9. IR (Nujol): 1324, 1160, 1121, 1095, 1065, 1017, 836, 780, 768, 723 cm^{-1}. Anal. Calcd for $C_{32}H_{38}N_2F_3ZrIr$: C, 48.58; H, 4.84; N, 3.54. Found: C, 48.68; H, 4.94; N, 3.50.

$Cp_2Zr(\mu$-N-^{t}Bu)(μ-NCH(*p*-$(MeO)C_6H_4)CH_2$-η^5-$C_5Me_4)Ir$ (2e). The procedure used to prepare **2c** was followed using 49.5 mg (7.98×10^{-5} mol) of $Cp_2Zr(\mu$-N-^{t}Bu)IrCp* and 10.7 mg (8.04×10^{-5} mol) of 4-methoxybenzonitrile in 8 mL of toluene. The solution turned to a greenish blue color after 3 h. The volatile materials were removed under reduced pressure, and the resulting solid was crystallized from 4 mL of a 1:1 pentane−toluene mixture. Blue crystals were obtained in 73% yield (43.9 mg, 5.83×10^{-5} mol). ^{1}H NMR (C_6D_6): δ 7.66 (d, 2, $J = 8.5$), 7.03 (d, 2, $J = 8.5$), 6.32 (dd, 1, $J = 5$, 10.5), 5.77 (s, 5), 5.67 (s, 5), 3.43 (s, 3), 3.14 (dd, 1, $J = 10.5$, 14.0), 2.66 (dd, 1, $J = 5.5$, 14.0), 1.63 (s, 3), 1.63 (s, 9), 1.56 (s, 3), 1.54 (s, 3), 1.51 (s, 3). ^{13}C{^{1}H} NMR (C_6D_6): δ 159.6, 142.3, 129.4, 114.2, 108.7, 108.0, 100.5, 96.5, 93.6, 91.6, 81.7, 81.0, 70.0, 55.2, 38.6, 35.4, 12.4, 12.0, 11.1, 10.7. IR (Nujol): 1542, 1260, 1191, 1150, 1088, 1017, 782 cm^{-1}. Anal. Calcd for $C_{32}H_{41}ON_2ZrIr$: C, 51.03; H, 5.49; N, 3.72. Found: C, 50.81; H, 5.29; N, 3.72.

$Cp_2Zr(\mu$-N-^{t}Bu)(μ-NCH(C_3H_5)CH_2-η^5-$C_5Me_4)Ir$ (2f). A solution of 98.7 mg (1.59×10^{-4} mol) of $Cp_2Zr(\mu$-N-^{t}Bu)IrCp* and 20 μL (2.72×10^{-4} mol) of cyanocyclopropane was prepared in 8 mL of toluene. The solution turned to a greenish blue color after 8 h. The volatile materials were removed under reduced pressure, and the solid was crystallized from 6 mL of a 1:1 pentane−toluene mixture. This resulted in blue crystals in 73% yield (79.7 mg, 1.16×10^{-4} mol). ^{1}H NMR (C_6D_6): δ 5.85 (s, 5), 5.79 (s, 5), 4.67 (m, 1), 2.80 (dd, 1, $J = 14.1, 10.2$), 2.63 (dd, 1, $J = 13.8, 5.71$), 1.63 (s, 9), 1.57 (s, 3), 1.55 (s, 3), 1.47 (s, 3), 1.36 (s, 3) 1.11 (t, 1, $J = 6.9$), 0.67 (m, 2), 0.4 (m, 1), 0.24 (m, 1). ^{13}C{^{1}H} NMR (C_6D_6): δ 108.2, 107.5, 98.8, 97.0, 95.1, 88.8, 82.5, 79.8, 69.1, 35.7, 35.1, 23.1, 11.8, 11.5, 10.9, 10.3, 6.2, 4.4. IR (Nujol): 2764, 2718, 1346, 1306, 1278, 1192, 1122, 1013, 916, 773, 707 cm^{-1}. Anal. Calcd for $C_{28}H_{39}N_2ZrIr$: C, 48.95, H, 5.72, N, 4.08. Found. C, 49.13, H, 5.38, N, 4.46.

^{1}H−^{1}H TOCSY Spectrum of $Cp_2Zr(\mu$-NCH(C_3H_5)(μ-N-^{t}Bu)Ir(CH_2-η^5-$C_5Me_4)$ (5). A solution was made up of 3.9×10^{-2} M $Cp_2Zr(\mu$-N-^{t}Bu)IrCp* (12 mg, 1.9×10^{-5} mol), 3.3×10^{-1} M cyanocyclopropane (11.2 mg, 1.67×10^{-4} mol), and 0.5 mL of toluene-d_8. The solution was immediately cooled to −78 °C. The reaction was allowed to proceed in the probe of a Bruker AMX300 instrument at 15 °C and was monitored by ^{1}NMR until the ratio of starting material to intermediate to product was approximately 1:2:1. The solution was then cooled to −60 °C. A ^{1}H−^{1}H TOCSY (total correlation spectroscopy) spectrum was acquired. For each of the 256 experiments, 4 scans were acquired and averaged, taking 1024 complex points with an acquisition time of 0.14 s, a relaxation delay of 1.0 s, and a mixing time of 37.7 ms using the MLEVTP sequence for mixing. A spectral width of 3600 Hz was used.

$Cp_2Zr(\mu$-N-^{t}Bu)(μ-NCH($CHMe_2$)CH_2-η^5-$C_5Me_4)Ir$ (2g). A reaction flask was charged with $Cp_2Zr(\mu$-N-^{t}Bu)IrCp* (84.8 mg, 1.37×10^{-4} mmol), dimethylacetonitrile (9.45 mg, 1.37×10^{-4} mmol), and 8 mL of toluene. The solution turned green upon heating at 75 °C for 8 h. The volatile materials were removed under reduced pressure, and the resulting solid was crystallized from 5 mL of diethyl ether to give blue crystals in 83% yield (78.6 mg, 1.14×10^{-4} mol). ^{1}H NMR (C_6D_6): δ 5.85 (s, 5), 5.77 (s, 5), 5.31 (m, 1) 2.73 (dd, 1, $J = 10$, 14), 2.33 (dd, 1, $J = 6$, 13.5), 2.24 (m, 1) 1.62 (s, 9), 1.58 (s, 3), 1.545 (s, 3), 1.50 (s, 3), 1.45 (s, 3), 1.36 (d, 3, $J = 7$), 1.18 (d, 3, $J = 7$). ^{13}C{^{1}H} NMR (C_6D_6): δ 108.6, 107.7, 101.8, 98.8, 93.2, 91.5, 82.2, 81.1, 69.6, 40.5, 35.4, 27.87, 23.4, 17.4, 12.3, 11.9, 11.1, 10.5. IR (Nujol): 1607, 1508, 1347, 1302, 1279, 1251, 1191, 1096, 1022, 773 cm^{-1}. Anal. Calcd for $C_{28}H_{41}N_2ZrIr$: C, 48.80; H, 6.00; N, 4.07. Found: C, 48.53; H, 5.90; N, 3.86.

$Cp_2Zr(\mu$-N-^{t}Bu)(μ-NCH($(CH_2)_3CN$)CH_2-η^5-$C_5Me_4)Ir$ (2h). A reaction flask was charged with $Cp_2Zr(\mu$-N-^{t}Bu)IrCp* (55.6 mg, 8.97×10^{-5} mol), 1,5-dicyanopentane (8.5 mg, 9.0×10^{-5} mol), and 5.0 mL of toluene. The solution turned aquamarine after heating for 8 h at 75 °C. The volatile materials were removed under reduced pressure, and the resulting solid was crystallized from 5 mL of diethyl ether to give blue crystals in 65% yield (41.6 mg, 5.83×10^{-5} mol). ^{1}H NMR (C_6D_6): δ 5.78 (s, 5), 5.76 (s, 5), 5.11 (m, 1), 2.32 (dd, 2, $J = 13.5$, $J = 29$), 2.31 (dd, 2, $J = 13.5$, 33), 1.88 (m, 2), 1.75 (m, 2), 1.61 (s, 9), 1.58 (s, 3), 1.55 (s, 3), 1.47 (s, 3), 1.37 (m, 2), 1.33 (s, 3). ^{13}C-{^{1}H} NMR (C_6D_6): δ 119.9, 108.6, 107.9, 100.8,, 94.9, 91.0, 90.2, 82.4, 80.5, 69.6, 43.9, 35.4, 35.3, 25.2, 17.8, 12.2, 11.9, 11.1, 10.7. IR (Nujol): 2244, 1191, 1117, 1012, 773 cm^{-1}. HRMS: *m*/*z* 713.1911 (M^+), calcd for $C_{19}H_{40}N_3ZrIr$ 713.1899.

$Cp_2Zr(\mu$-N-^{t}Bu)(μ-NCH(CH_2Ph)CH_2-η^5-$C_5Me_4)Ir$ (4a). In the drybox, a reaction flask was charged with 95.6 mg (1.54×10^{-4} mol) of $Cp_2Zr(\mu$-N-^{t}Bu)IrCp* and 10 mL of toluene. Phenylacetonitrile (20.5 μL, 1.78×10^{-4} mol) was added via syringe. The bomb was sealed and immediately put into a 75 °C bath for 8 h. The volatile material was removed at room temperature in vacuo. Blue crystals were obtained in 72% yield

from 6 mL of a 1:1 toluene−pentane mixture at −30 °C (81.7 mg, 1.11 × 10^{-4} mol). ^{1}H NMR (C_6D_6): δ 7.39 (d, 2, J = 7), 7.29 (t, 2, J = 7.5), 6.81 (t, 1, J = 7.5), 5.85 (s, 5), 5.83 (s, 5), 5.66 (m, 1), 3.52 (m, 1), 3.17 (dd, 1, J = 11, 13.5), 2.57 (dd, J = 13.5, 63.5), 2.55 (dd, 1, J = 13.5, 59.0), 1.62 (s, 9), 1.53 (s, 3), 1.51 (s, 3), 1.39 (s, 3), 1.36 (s, 3). ^{13}C{^{1}H} NMR (C_6D_6): δ 14.6, 129.5, 129.2, 126.8, 108.7, 107.9, 100.9, 95.0, 94.2, 90.1, 82.5, 80.6, 69.6, 53.1, 35.7, 35.4, 12.2, 11.9, 11.2, 10.6. Anal. Calcd for $C_{32}H_{41}N_2ZrIr$: C, 52.14; H, 5.61; N, 3.80. Found: C, 52.12; H, 5.44; N, 3.80.

$Cp_2Zr(\mu$-N-^{t}Bu)(μ-N-CHCH(Ph))IrCp* (5a). In the drybox, 253 mg (4.07 × 10^{-4} mol) of $Cp_2Zr(\mu$-N-^{t}Bu)IrCp* was dissolved in 10 mL of toluene. Phenylacetonitrile (0.50 mL, 4.33 × 10^{-3} mol) was added via syringe. The solution was stirred for 5 min and was then left standing for 8 h. The toluene was removed at room temperature in vacuo. The remaining solution (the product dissolved into the high-boiling phenylacetonitrile) was washed three times with 5 mL of pentane to remove the phenylacetonitrile. The solid was reddish brown after the removal of the nitrile. The solid was washed three times with diethyl ether and then dissolved in 2 mL of THF. The solution was cooled to −30 °C for 3 days. Green solid precipitated out of the solution (19.6 mg, 2.66 × 10^{-5} mol, 6.5%). ^{1}H NMR (C_6D_6): δ 8.82 (d, 1, J = 12.8), 7.72 (m, 2), 7.42 (m, 3), 6.20 (d, 1, J = 12.8), 5.88 (s, 10), 1.60 (s, 9), 1.34 (s, 15). ^{13}C{^{1}H} NMR (C_6D_6): δ 157.9, 142.4, 129.0, 123.6, 122.2, 109.6, 87.9, 68.0, 35.5, 10.1. HRMS: m/z 736.1947 (M^+), calcd for $C_{32}H_{41}N_2ZrIr$ 736.1946.

$Cp_2Zr(\mu$-N-^{t}Bu)(μ-N-CHCH(p-$CF_3C_6H_4$))IrCp* (5b). In the drybox, 179 mg (2.88 × 10^{-4} mol) of $Cp_2Zr(\mu$-N-^{t}Bu)IrCp* was dissolved into 4 mL of toluene. To this was added a solution consisting of 53.3 mg (2.88 × 10^{-4} mol) of (4-(trifluoromethyl)phenyl)acetonitrile and 2 mL of toluene. The solution turned green after 30 min at room temperature. After 1 day the volatile material was removed at room temperature in vacuo and the resulting dark green solid was crystallized from a 1:1 toluene−pentane mixture at −30 °C (75.3 mg, 93.5 × 10^{-5} mol, 32.5%). ^{1}H NMR (C_6D_6): δ 8.81 (d, 1, J = 12.5), 7.59 (d, 1 J = 8.5), 7.41 (d, 1, J = 8.5), 5.95 (d, 1, J = 5.83), 1.56 (s, 9), 1.31 (s, 15). ^{13}C{^{1}H} NMR (C_6D_6): δ 161.1, 146.8, 126.6, 121.0, 108.7, 91.6, 96.1, 36.0, 30.1. Anal. Calcd for $C_{33}H_{40}F_3N_2ZrIr$: C, 49.23; H, 5.01; N, 3.48. Found: C, 49.59; H, 5.20; N, 3.74.

X-ray Structure Determination of Complex 5b. An orange bladelike crystal was obtained by slow cooling of a saturated toluene solution form 25 to −30 °C. The crystal was mounted on a glass fiber using Paratone N hydrocarbon oil. It was cooled to −122 ± 1 °C by a nitrogen-flow low-temperature apparatus which had been previously calibrated by a thermocouple placed at the sample position. Crystal quality was evaluated via measurement of intensities and inspection of peak scans. All measurements were made on a SMART CCD are detector. The crystal data can be found in Table 4. Cell constants and an orientation matrix, obtained from a least-squares refinement using the measured positions of 6231 reflections in the range 3.00 < 2θ < 46.00°, corresponded to a primitive orthorhombic cell. The final cell parameters and specific data collection parameters for this data set are given in the Supporting Information.

Data were integrated to a maximum 2θ value of 49.4°. The data were corrected for Lorentz and polarization effects. No correction for crystal decomposition was necessary. Data were analyzed for agreement and possible adsorption. An empirical absorption correction based on comparison of redundant and equivalent reflections was applied (T_{max} = 0.96, T_{min} = 0.53). The structure was solved by direct methods and expanded using Fourier techniques. The Ir, Zr, and F atoms were refined anisotropically, while the rest were refined isotropically. Attempts to refine the carbon and nitrogen atoms anisotropically led to unreasonable values for the components of the anisotropic displacement parameters. These problems are most likely a result of the extremely asymmetric shape of the crystal. In addition, there was also evidence of a small crystal fragment attached to the main crystal. This would cause small but systematic errors in the structure factors. Hydrogen atoms were included in calculated idealized positions but not refined. The maximum and minimum peaks on the final difference Fourier map corresponded to 3.40 and −3.81 e/Å^3, respectively. The positional and anisotropic thermal parameters are given in the Supporting Information.

$Cp_2Zr(\mu$-N-^{t}Bu)(μ-NCHCH$_2$(p-MeOC$_6$H$_4$)CH$_2$-η^5-C$_5$Me$_4$)-Ir (4c). A reaction flask was charged with $Cp_2Zr(\mu$-N-^{t}Bu)-IrCp* (115.5 mg, 1.86 × 10^{-4} mol), (4-methoxyphenyl)-acetonitrile (25.3 μL, 1.86 × 10^{-4} mo), and 20 mL of toluene. The solution turned green upon heating at 75 °C for 8 h. The volatile materials were removed under reduced pressure, and the resulting solid was crystallized from 5 mL of diethyl ether to give blue crystals in 69% yield (98.4 mg, 1.28 × 10^{-4} mol). ^{1}H NMR (C_6D_6): δ 7.32 (d, 2, J = 8.5), 7.15 (d, 2, J = 8.5), 5.84 (s, 5), 5.83 (s, 5), 5.65 (m, 1), 3.51 (dd, 1, J = 3.5, 13), 3.15 (dd, 1, J = 10.5, 13), 2.60 (dd, 1, J = 13.5, 36), 2.59 (dd, 1, J = 13.5, 45) 1.62 (s, 9), 1.55 (s, 3), 1.53 (s, 3), 1.42 (s, 3), 1.41 (s, 3). ^{13}C{^{1}H} NMR (C_6D_6): δ 159.1, 134.7, 130.35, 114.7, 108.7, 107.9, 101.0, 95.0, 94.6, 90.1, 82.6, 80.6, 69.6, 55.2, 52.2, 35.8, 35.4, 12.2, 11.9, 11.2, 10.6. Anal. Calcd for $C_{33}H_{43}ON_2ZrIr$: C, 51.03; H, 5.49; N, 3.72. Found: C, 50.81; H, 5.27; N, 3.58.

$Cp_2Zr(\mu$-N-^{t}Bu)(μ-N-CHCH(p-MeOC$_6$H$_4$))IrCp* (5c). In the drybox, 238 mg (3.84 × 10^{-4} mol) of $Cp_2Zr(\mu$-N-^{t}Bu)IrCp* was dissolved into 4 mL of toluene. To this was added a solution consisting of (4-methoxyphenyl)acetonitrile (491 mg, 3.34 × 10^{-3} mol) and 2 mL of toluene. The solution turned green after 8 h. After 1 day, the solution was filtered through glass fiber and the volatiles were removed under reduced pressure. The remaining solution was washed three times with 7 mL of cold pentane to remove the (4-methoxyphenyl)-acetonitrile. The solid was then dissolved into 2 mL of toluene and cooled for 3 days at −30 °C to give 19.6 mg of a dark green solid (2.55 × 10^{-5} mol, 7%). ^{1}H NMR (C_6D_6): δ 8.70 (d, 1, J = 13), 7.66 (d, 2, J = 8.5), 7.05 (d, 2, J = 8.5), 6.24 (d, 1, J = 13), 5.89 (s, 10), 3.49 (s, 3), 1.63 (s, 9), 1.38 (s, 15). ^{13}C{^{1}H} NMR (C_6D_6): 135.6, 127.6, 121.3, 120.1, 111.6, 110.9, 93.1, 87.6, 67.1, 36.7, 9.8. HRMS: m/z 766.2051 (M^+), calcd for $C_{33}H_{43}N_2OZrIr$ 766.2052.

Kinetics Study of the Reaction of 1 with 2-Arylacetonitriles. General Procedure: ^{1}H NMR Spectroscopy. A stock solution was prepared using 32.1 mg (5.18 × 10^{-5} mol, 1.62 × 10^{-2} M) of $Cp_2Zr(\mu$-N-^{t}Bu)IrCp* and 26.5 mg (1.61 × 10^{-4} mol, 5.02 × 10^{-2} M) of 1,3,5-trimethoxybenzene (internal standard). The solution was stored in the drybox at −30 °C between uses.

In a typical run, a Teflon-capped NMR tube was charged with 500 ± 5 μL of stock solution #1. A 10.0 ± 0.05 μL amount of (4-methoxyphenyl)acetonitrile was added, and the solution was immediately cooled to −78 °C. The calculated concentration of 2-arylacetonitrile used was 1.47 × 10^{-2} M. The sample was allowed to equilibrate at 25 °C for 2 min in the probe of a Bruker AMX300 instrument. Single-scan spectra were obtained at intervals of 90 s. The FID data sets were all transformed and phased. An automatic baseline correction was applied to each spectrum. The Cp peaks of **1**, **4c**, and **5c** were integrated against phenyl protons of the internal standard ($C_6H_3(OMe)_3$). The integration data was transferred into Microsoft Excel for analysis.

General Procedure: UV−vis Spectroscopy. UV−vis spectrometry was used to study the rate of the reaction of $Cp_2Zr(\mu$-N-^{t}Bu)IrCp* plus (p-X-phenyl)acetonitrile (X = H, MeO, CF_3). Preliminary results indicated the need for the oxygen/water scavenger Cp_2ZrMe_2. To verify that Cp_2ZrMe_2 would not affect the reaction of **1** plus 2-arylnitriles, an NMR tube was charged with 5 mg of $Cp_2Zr(\mu$-N-^{t}Bu)IrCp* (8.1 × 10^{-6} mol, 1.6 × 10^{-2} M), 10.0 μL of (4-methoxyphenyl)acetonitrile (7.37

$\times 10^{-4}$ mol, 1.5×10^{-1} M), 3.0 mg (1.19×10^{-5} mol, 2.39×10^{-2} M) of Cp_2ZrMe_2, and 0.50 mL of C_6D_6. No difference in rate or product distribution between the two tubes was observed.

A stock solution was prepared by charging a 25.0 mL volumetric flask with 19.8 mg (3.19×10^{-5} mol, 1.27×10^{-3} M) of $Cp_2Zr(\mu\text{-N-}^t\text{Bu})IrCp^*$, 10.1 mg ($4.0 \times 10^{-5}$ mol, 1.61×10^{-3} M) of Cp_2ZrMe_2, and enough benzene to bring the total volume to 25.0 mL. The benzene used was freshly distilled and stored in a glass bomb to prevent contamination. A stock solution of (4-(trifluoromethyl)phenyl)acetonitrile was prepared by charging a 5.00 mL volumetric flask with 126 mg (6.79×10^{-4} mol, 1.35×10^{-1} M) of (4-(trifluoromethyl)phenyl)-acetonitrile and enough benzene to bring the total volume to 5.00 mL.

In a typical run, a cuvette was charged with 1.00 mL of the metal solution, 0.50 mL of the nitrile solution, and 0.50 mL of benzene to make a final volume of 2.00 mL. All solutions were transferred via volumetric pipet. The calculated concentrations were 6.35×10^{-4} M $Cp_2Zr(\mu\text{-N-}t\text{-Bu})IrCp^*$, 8.05×10^{-4} M Cp_2ZrMe_2, and 3.38×10^{-2} M (4-(trifluoromethyl)phenyl)acetonitrile.

The sample was allowed to equilibrate at 25 ± 1 °C for 2 min in the spectrometer. A spectrum was then obtained every 30 s. The change of absorbance at 650 nm was monitored and analyzed in the same manner as the ^{1}H NMR spectrometry data.

Product Ratio Determination. ^{1}H NMR spectroscopy was used to analyze the product ratio from the reaction of $Cp_2Zr(\mu\text{-N-}^t\text{Bu})IrCp^*$ with 2-arylacetonitriles. In a typical run, a stock solution was made of 23.2 mg (1.28×10^{-4} mol, 1.61×10^{-2} M) of $Cp_2Zr(\mu\text{-N-}^t\text{Bu})IrCp^*$ and 1.86 mL of C_6D_6. A second stock solution was made of 1.89×10^{-1} g (1.61×10^{-3} mol) of phenylacetonitrile. Four NMR tubes with Teflon caps were charged with 400 ± 5 μL of the stock solution. Varying amounts of the phenylacetonitrile stock solution (100, 50, 25, and 5 μL) were added to each tube, and additional C_6D_6 (0, 50, 75, and 95 μL) was syringed into each tube to make a final volume of 500 μL. The tubes were allowed to sit at 25 °C for 3 days. An eight-pulse spectrum, with 60 s delay to allow for complete proton relaxation, was then acquired on each of the tubes. The Cp resonances of **5a** (δ 5.88 ppm) and **4a** (δ 5.85 and 5.83) were integrated, and the ratio of **5a** to **4a** was calculated from these values.

Product Ratio Determination of $Cp_2Zr(\mu\text{-N-}^t\text{Bu})(\mu\text{-N-CHCH}(p\text{-MeOC}_6H_4))IrCp^*$ (5c):$Cp_2Zr(\mu\text{-N-}^t\text{Bu})(\mu\text{-NCH-}(CH_2(p\text{-MeOC}_6H_4))CH_2\text{-}\eta^5\text{-}C_5Me_4)Ir$ (4c) with Added "Effector". General Procedure: Preliminary Results. In a typical run, a stock solution was made of 2.48×10^{-2} g (4.00×10^{-4} mol. 1.61×10^{-2} M) of $Cp_2Zr(\mu\text{-N-}^t\text{Bu})IrCp^*$ and 1.98 mL of C_6D_6 (via 1.00 ± 0.05 mL syringe). A second stock solution was made of 21.6 mg (1.46×10^{-4} mol, 1.60×10^{-2} M) and 0.916 mL of C_6D_6. A vial was charged with 9.5 mg of methyl phenylacetate and 50.0 μL of C_6D_6. A 400 μL amount of the metal-containing stock solution was transferred, followed by 50.0 μL of the nitrile solution. The resulting solution was transferred to an NMR tube with a Teflon cap and allowed to stand for 4 days. The product ratio (**5c**:**4c**, 0.41) was determined using the same procedure described above.

General Procedure: Generation of an "Effector" Plot. The product ratio of the reaction of $Cp_2Zr(\mu\text{-N-}^t\text{Bu})IrCp^*$ with (4-methoxyphenyl)acetonitrile with added effector was analyzed by ^{1}H NMR spectroscopy. In a typical run, stock solutions were made of 2.57×10^{-2} g (4.15×10^{-5} mol) of $Cp_2Zr(\mu\text{-N-}^t\text{Bu})IrCp^*$ and 2.06 mL of C_6D_6, 2.17×10^{-2} g (1.47×10^{-4} mol) of (4-methoxyphenyl)acetonitrile and 0.916 mL of C_6D_6, and 4.26×10^{-2} g (1.95×10^{-4} mol) of 4-(trifluoromethylphenyl)acetate and 1.20 mL of C_6D_6. Four NMR tubes with Teflon caps were charged with 50.0 μL of the nitrile solution, and varying amounts of the acetate stock solution (0, 10, 25, and 50 μL) were added to each tube. Additional C_6D_6 was added (50, 40, 25, and 0 μL) followed by 400 μL of the metal-containing stock solution. The solutions were allowed to sit for 4 days at 25 °C. The **5c**:**4c** ratio was determined using the procedure described above.

Reaction of 1- and 2-Arylacetonitriles-d_2: General Method. In a typical experiment, an NMR tube previously treated with 1,1,3,3-hexamethyldisilazane was then charged with 5.0 mg (8.2×10^{-6} mol, 1.6×10^{-2} M) of $Cp_2Zr(\mu\text{-N-}^t\text{Bu})IrCp^*$, 10 μL (8.5×10^{-4} mol, 1.7×10^{-1} M) of $PhCD_2CN$, and 0.50 mL of C_6D_6. Deuterium incorporation into **4a-d_2** and **5a-d_2** was observed after 1 day by ^{1}H NMR spectrometry, which showed no detectable resonances at δ 6.20, 3.54, and 3.17 and a singlet instead of a doublet at δ 8.82. The volatile materials were removed under reduced pressure, and the solids were dissolved in C_6H_6. ^{2}H NMR spectroscopy revealed four new resonances (other than $PhCD_2CN$) at δ 6.20, 3.54, and 3.17 and in the Cp* ring of **5a-d_2** at δ 1.34.

Reaction of 1 and $PhCD_2CN$ and (4-Methoxyphenyl)-acetonitrile. A silylated NMR tube was charged with 10.0 mg (1.61×10^{-5} mol) of $Cp_2Zr(\mu\text{-N-}^t\text{Bu})IrCp^*$, 5.0 μL (4.1×10^{-5} mol) of $PhCD_2CN$, and 5.0 μL (3.1×10^{-5} mol) of (4-methoxyphenyl)acetonitrile. The ^{1}H NMR spectrum taken after 1 day revealed two triplet-like resonances centered at δ 8.82 and 8.70, indicating deuterium and hydrogen incorporation into both **5a** and **5c**.

Preparation of 2-Arylacetonitriles-d_2. 2-Arylacetonitriles-d_2 were prepared by base-catalyzed (K_2CO_3) exchange of benzylic protons with D_2O. This procedure was repeated, and an average of 97% deuterium incorporation was observed by ^{1}H NMR spectroscopy.

Acknowledgment. We are grateful to the National Science Foundation (Grant No. CHE-9633374) for financial support. We also thank Dr. Frederick Hollander and Dr. Dana Caulder of the UC Berkeley College of Chemistry X-ray diffraction facility (CHEXRAY) for their crystallographic determinations.

Supporting Information Available: Tables giving details of the data collection and refinement and atomic coordinates and thermal parameters for complexes **2a** and **5b**, along with tables of bond lengths and bond angles for complex **5b**. This material is available free of charge via the Internet at http://pubs.acs.org.

OM990785L